Chalcogenide Letters Vol. 18, No. 7, July 2021, p. 397 - 403

Solvothermal synthesis, characterization and visible-light-driven photocatalysis of self-assembled flower-like CdS nanostructure

P. Intaphong[a], A. Phuruangrat[a,*], K. Akhbari[b], T. Sakhon[c], B. Kuntalue[c], T. Thongtem[d,e], S. Thongtem[d,f]

[a]*Division of Physical Science, Faculty of Science, Prince of Songkla University, Hat Yai, Songkhla 90112, Thailand*
[b]*School of Chemistry, College of Science, University of Tehran, Tehran, Iran*
[c]*Electron Microscopy Research and Service Center, Faculty of Science, Chiang Mai University, Chiang Mai 50200, Thailand*
[d]*Materials Science Research Center, Faculty of Science, Chiang Mai University, Chiang Mai 50200, Thailand*
[e]*Department of Chemistry, Faculty of Science, Chiang Mai University, Chiang Mai 50200, Thailand*
[f]*Department of Physics and Materials Science, Faculty of Science, Chiang Mai University, Chiang Mai 50200, Thailand*

Self-assembled nanorods/nanowires of CdS were successfully synthesized by a solvothermal method at 200 °C for 5, 10 and 20 h using sodium dodecylsulfonate as a capping reagent. X-ray diffraction (XRD) patterns of all CdS samples can be indexed to pure phase of hexagonal CdS structure. The degree of crystallinity of CdS was increased with the increase of holding reaction time from 5 h to 20 h. Transmission electron microscopic (TEM) images revealed that the product synthesized by the solvothermal method at 200 °C for 20 h contained self-assembled flower-like CdS nanostructure. The UV-visible absorption of self-assembled flower-like CdS nanostructure shows excellent absorption in UV-visible region with the absorption peak at 481 nm. Photocatalytic efficiency of the as-prepared CdS samples was investigated through rhodamine B (RhB) degradation under visible light irradiation. In this research, the self-assembled flower-like CdS nanostructure has the highest degradation of 94.91 % within 80 min.

(Received April 23, 2021; Accepted July 9, 2021)

Keywords: CdS; Stable photocatalyst; Nanomaterials; TEM

1. Introduction

In 1972, Fujishima and Honda reported the use of titanium dioxide (TiO_2) photoanode for water splitting in a photoelectrochemical cells (PEC) under UV light irradiation [1-3]. The TiO_2 semiconductor photocatalyst is the most widely used for water splitting and photodegradation of toxic organic chemicals in wastewater and air pollution because it is high chemical stability, low cost and strong redox ability [1, 2, 4]. Moreover, application of TiO_2 was limited and active only under UV light irradiation because of its wide band gap and high recombination rate of electron-hole pairs [1, 2]. Thus, the visible-light-driven photocatalyst has become a wide application in recent years due to the utilization of visible light of about 45% of solar radiation with its energy < energy of UV light (~4%) [5, 6].

Cadmium sulfide (CdS) as one of the most important II–VI semiconductor with direct band gap of 2.4 eV has wide potential application in optoelectronic and luminescence such as photodetectors, solar cells, lasers, high-density magnetic information storages and photocatalysts [7-11]. CdS photocatalyst has been intensively utilized for conversion of solar energy into chemical energy and for photodegradation of organic chemicals including rhodamine B (RhB) [5, 7, 9, 10], methyl violet (MV) [7], methylene blue (MB) [7, 11, 12], malachite green (MG) [7, 13], reactive red azo dye (RR141) [8] and methyl orange (MO) [7, 14, 15] containing in wastewater

* Corresponding author: phuruangrat@hotmail.com

https://doi.org/10.15251/CL.2021.187.397

under visible light irradiation because conduction band edge of CdS is more negative than the reduction potential of proton. In addition, CdS has sufficient absorption coefficient and relatively narrow band gap with effective photocatalytic activity [3, 14, 16].

In this research, self-assembled flower-like CdS nanostructure was synthetized by solvothermal method using sodium dodecylsulfonate as a capping reagent. Phase, morphology and optical property of as-prepared CdS were investigated by X-ray powder diffraction (XRD), Raman spectrophotometry, transmission electron microscopy (TEM) and UV-visible spectroscopy. Photocatalytic performance of self-assembled flower-like CdS nanostructure was studied through rhodamine B (RhB) degradation under visible radiation.

2. Experiment

All chemicals with analytical grade were used without further purification. In this experiment, 0.0050 mol $Cd(NO_3)_2 \cdot 5H_2O$ and 0.0075 mol thioglycolic acid (TGA) were dissolved in 100 ml of ethylenediamine solvent. Then, 0.25 g sodium dodecylsulfonate as a capping reagent was added in the mixed solution with 30 min stirring. Every solution was put in 150 ml Teflon-lined stainless steel autoclaves and heated in an oven at 200 ^oC for 5, 10 and 20 h. In the end, bright yellow precipitates were collected, washed with distilled water and absolute ethanol, and dried for further characterization.

Phase and structure of as-prepared samples were analyzed by a Philips X'Pert MPD X-ray powder diffractometer (XRD) using Cu-K_α as an X-ray source at 10^o-60^o. Raman spectrum was recorded on a HORIBA Jobin Yvon T64000 Raman spectrometer at 50 mW and 514.5 nm wavelength Ar green laser in the wavenumber range of 200-800 cm^{-1}. Morphologies of the samples were observed through a JEOL JEM-2010 transmission electron microscope (TEM) at an accelerating voltage of 200 kV. Optical absorbance of a sample was analyzed by Lambda 25 Perkin Elmer UV-visible spectroscopy at wavelength of 200-800 nm.

Photocatalytic activities of the as-prepared samples were investigated through rhodamine B (RhB) degradation under visible light irradiation. 0.2 g of the as-synthesized sample was added in 200 ml $1x10^{-5}$ M RhB solution which was stirred for 30 min in the dark to develop adsorption–desorption equilibrium. Then, the solution was illuminated by visible light irradiation and about 5 ml RhB solution was withdrawn every 20 min and centrifuged to remove the as-prepared sample. The concentration of RhB was measured by a UV-visible spectrophotometer at λ_{max} of 554 nm. The degradation efficiency was calculated by the following equation.

$$\text{Decolorization efficiency (\%)} = \frac{C_o - C_t}{C_o} x100 \quad (1)$$

, where C_o is the initial concentration at 0 min and C_t is the concentration at a time t min.

3. Results and discussion

Phase of as-prepared CdS nanostructure was analyzed by XRD (Fig. 1). The patterns can be indexed to hexagonal CdS nanostructure of the JCPDS database no. 41-1049 [17]. The XRD patterns of only the as-prepared samples synthesized by solvothermal method at 200 ^oC for 10 and 20 h showed diffraction peaks at 2θ of 24.74^o, 26.43^o, 28.10^o, 36.69^o, 43.81^o, 47.89^o, 50.61^o, 51.97^o and 52.81^o which were identified to the (100), (002), (101), (102), (110), (103), (200), (112) and (201) crystallographic planes of hexagonal CdS phase, respectively. The intensities of as-prepared CdS samples were increased with the increase of prolonged period of reaction time. Thus, the degree of crystallinity was improved [9, 18].

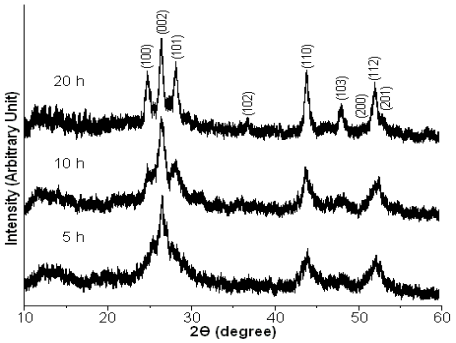

Fig. 1 X-ray diffraction patterns of as-prepared CdS samples synthesized by solvothermal method at 200 ^{o}C for 5, 10 and 20 h.

All XRD patterns of as-prepared CdS nanostructure samples show broad diffraction peaks, suggesting that the crystalline samples were in nanoscale size controlled by the efficiency of capping activity of sodium dodecylsulfonate [19, 20]. The mean size of the ordered (crystalline) domains which may be smaller or equal to the grain size or particle size (D) of sample was calculated by Scherrer equation as follows.

$$D = K\lambda/\beta\cos\theta \quad (2)$$

K is the dimensionless shape factor with a value close to unity. The shape factor has a typical value of about 0.9 but it varies with the real shape of the crystal, λ is the Cu-K_α X-ray wavelength, β is the line broadening at half maximum intensity (FWHM) without instrumental line broadening and θ is the Bragg diffraction angle [8, 11, 14, 21]. The mean crystallite sizes of the samples are 13.75, 15.32, and 18.53 nm for the solvothermal synthesis at 200 ^{o}C for 5, 10 and 20 h, respectively.

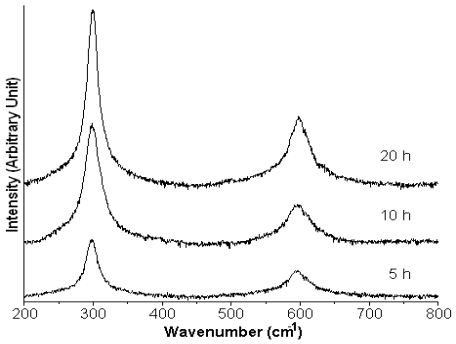

Fig. 2 Raman spectra of as-prepared CdS samples synthesized by solvothermal method at 200 ^{o}C for 5, 10 and 20 h.

Fig. 2 shows Raman spectra of the as-obtained CdS nanostructure samples prepared by solvothermal method at 200 ^{o}C for 5, 10 and 20 h over wavenumber range of 200-800 cm^{-1}. By group theory analysis, hexagonal wurtzite CdS belongs to C^4_{6v} space group containing two formula units per primitive cell with all atoms occupy the site of C_{3v} symmetry [22, 23]. At the center (Γ) of the Brillouin zone of hexagonal wurtzite CdS structure predicts the optical phonon vibration.

$$\Gamma_{opt} = 1A_1(TO) + 1A_1(LO) + 1E_1(TO) + 1E_1(LO) + 2E_2 \quad (3)$$

, where $1A_1 + 1E_1 + 2E_2$ (E_{2H} and E_{2L}) modes are Raman active, but $2B_2$ modes are silent [9, 22, 23]. They correspond with the longitudinal-optical (LO) and transverse-optical (TO) phonon

modes in A_1 and E_1 modes [9, 22, 23]. The phonon polarization of A_1 branch is in the [001] direction while the phonon polarization of E_1 and E_2 branches are in the (001) plane [22, 23]. Raman spectra of as-prepared CdS nanostructure samples show the Raman peaks located at 298 and 596 cm^{-1} which are attributed to the first and second order longitudinal-optical phonon modes of hexagonal wurtzite CdS structure, respectively [9, 11, 22].

Fig. 3 shows TEM images, SAED pattern and HRTEM image of the as-obtained CdS nanostructure samples prepared by solvothermal method at 200 ^oC for 5, 10 and 20 h. The TEM image of as-obtained CdS sample solvothermally prepared at 200 ^oC for 5 h shows that the sample was composed of CdS nanorods oriented in different directions. When the reaction time was prolonged to 10 and 20 h, CdS nanorods grew out of the central points to form microflowers. When the prolonged reaction time was 20 h, the as-prepared CdS sample contained microflowers of self-assembled nanowires with 2–3 μm long and 50 nm diameter. A selected-area electron diffraction (SAED) pattern of single CdS nanowire presents bright spots of electron diffraction. The as-obtained CdS nanowire is single crystal. The pattern was indexed to the (110), (112) and (002) crystalline planes of hexagonal wurtzite CdS structure. A high resolution transmission electron microscopic (HRTEM) image of single CdS nanowire shows the interplanar space of 0.336 nm corresponding to the (002) plane of hexagonal wurtzite CdS structure. These results certified that growth of CdS nanowire was in the [001] direction [5, 9, 11].

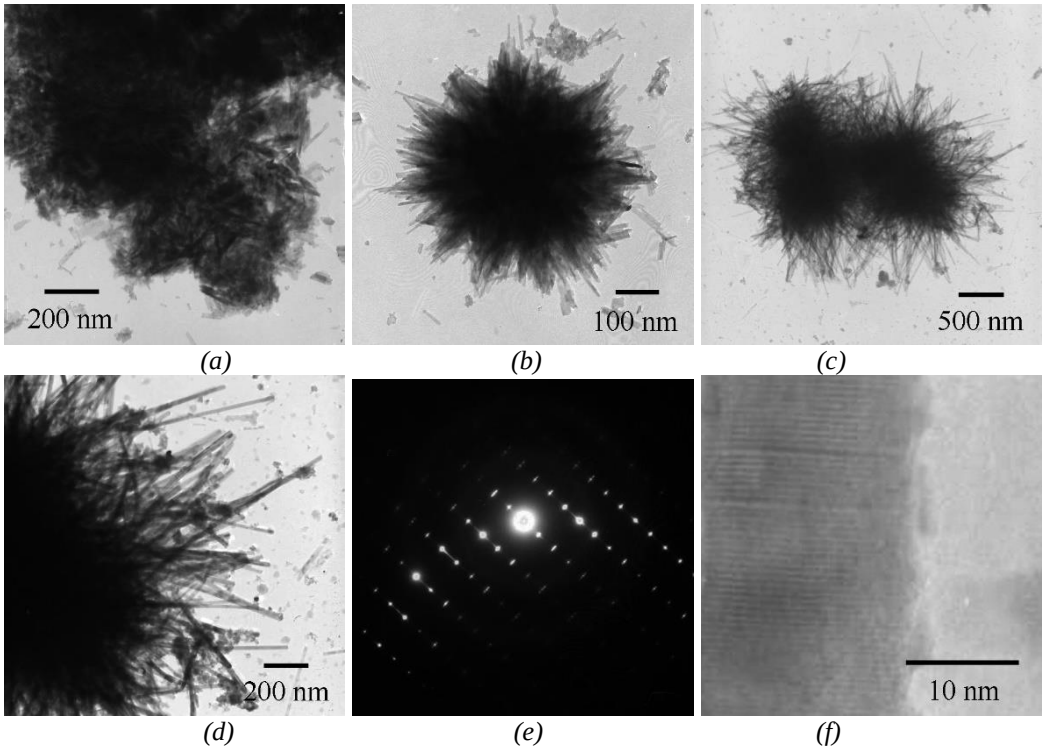

Fig. 3 TEM images, SAED pattern and HETEM image of as-prepared CdS samples synthesized by solvothermal method at 200 ^oC for (a) 5 h, (b) 10 h and (c-f) 20 h.

The optical property of as-obtained CdS nanostructure samples prepared by solvothermal method at 200 ^oC for 20 h was investigated by UV-visible spectroscopy. Fig. 4 shows the UV-visible absorption of self-assembled flower-like CdS sample over the wavelength range of 250-800 nm. The excellent absorption in UV-visible region with an absorption peak at 481 nm and band edge of 516 nm for self-assembled flower-like CdS structure sample was detected [8, 10, 11, 14]. The band gap energy (E_g) of the self-assembled flower-like CdS structure sample was calculated by the following equation.

$$E_g\ (eV) = 1239.8031/\lambda_{(nm)} \quad (4)$$

, where λ is the wavelength of band edge [24, 25]. The optical property of the as-obtained CdS nanostructure sample prepared by solvothermal method at 200 °C for 20 h is 2.40 eV which is red-shifted energy w.r.t. the energy gap of bulk CdS (2.42 eV) influenced by the quantum confinement effect of the nanowires [8, 10, 11, 14].

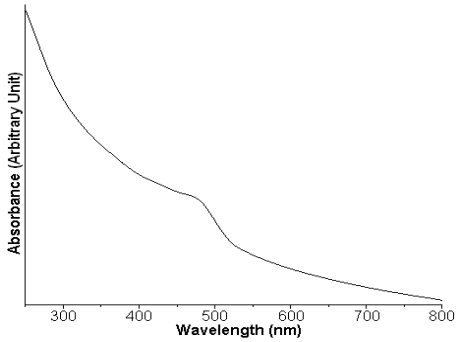

Fig. 4 UV-visible absorption of as-prepared CdS sample synthesized by solvothermal method at 200 °C for 20 h.

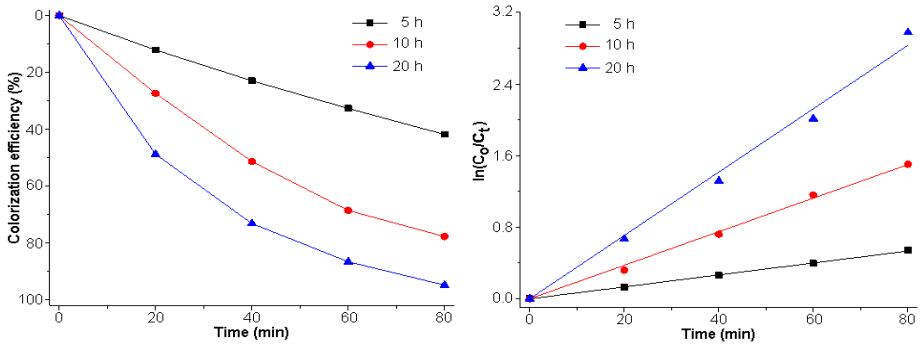

(a) *(b)*

Fig. 5 (a) Photodegradation efficiency and (b) reaction kinetics for RhB degradation over as-prepared CdS samples synthesized by solvothermal method at 200 °C for 5, 10 and 20 h under visible light irradiation.

The photocatalytic activities and the pseudo-first-order kinetics of as-obtained CdS nanostructure samples prepared by solvothermal method at 200 °C for 5, 10 and 20 h were investigated through the RhB degradation under visible light irradiation as the results shown in Fig. 5. The photodegradation of RhB over the as-prepared CdS samples synthesized at 200 °C for 5, 10 and 20 h are 41.89%, 77.77% and 94.91% within 80 min under visible light irradiation, respectively. The results indicate that the active species were produced during photocatalytic reaction and that RhB molecules were degraded into harmless organic compounds [7, 11, 14]. Photo-excited electrons and photo-induced holes resided in conduction band (CB) and valence band (VB) of CdS semiconductor under visible light irradiation [7, 11, 14]. The photo-excited electrons and photo-induced holes diffused to the surface of CdS at which adsorbed O_2 and OH^-/H_2O molecules were transformed into $^{\bullet}O_2^-$ and $^{\bullet}OH$ radicals [7, 11, 14]. Subsequently, RhB molecules were degraded and transformed into harmless organic compounds [7, 11, 14]. The RhB degradation over CdS samples under visible light irradiation can be expressed by the pseudo-first-order kinetics as follows.

$$\ln(C_o/C_t) = kt \quad (5)$$

, where C_o and C_t are the RhB concentrations at time 0 and t, k is the pseudo-first-order rate constant and t is the irradiation time of visible light [2, 9, 24]. The plots were fitted to a linear line, therefore, the RhB degradation over CdS nanomaterials corresponds to the pseudo-first-order kinetics [5, 9, 24]. The kinetic rate constants for RhB degradation over CdS samples synthesized at 200 ^{o}C for 5, 10 and 20 h are $6.62x10^{-3}$, 0.0187 and 0.0356 min^{-1}, respectively. In this research, CdS nanostructure sample synthesized by solvothermal method at 200 ^{o}C for 20 h has the highest rate constant for RhB degradation under visible light irradiation.

Photocatalytic stability and recyclability are the main parameters for practical application. The stability of the photocatalyst was evaluated through the recycled test for photodegradation of RhB over the reused self-assembled flower-like CdS sample synthesized at 200 ^{o}C for 20 h. The self-assembled flower-like CdS sample at the end of each photocatalytic cycle was collected, washed and dried for the next run. Fig. 6 shows the photocatalytic efficiencies for RhB degradation over the reused self-assembled flower-like CdS nanostructure within 5 cycles. The photocatalytic efficiency of the reused self-assembled flower-like CdS sample at the end of cycle five was decreased to 91.25 %. The result indicates that the self-assembled flower-like CdS sample is highly stable and is a promising material that can play the role in degrading treatment of RhB dye under visible light irradiation.

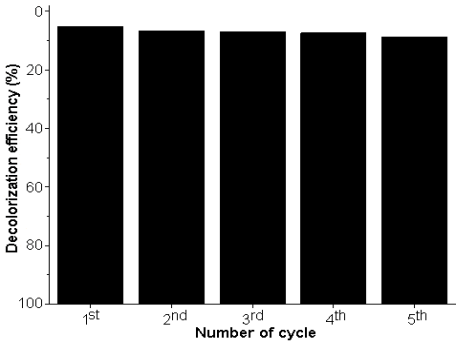

Fig. 6 The photocatalytic test of reused CdS nanostructure flowers used for RhB degradation under visible light irradiation.

4. Conclusions

Self-assembled flower-like CdS nanostructure sample was synthesized by a solvothermal method at 200 ^{o}C for 20 h. The XRD and TEM results show that the as-prepared sample synthesized by a solvothermal method at 200 ^{o}C for 20 h contained hexagonal CdS nanostructure of self-assembled nanowires with 2–3 μm long and 50 nm diameter to form microflowers. The photocatalytic activity of self-assembled flower-like CdS nanostructure in degrading of RhB within 80 min under visible light irradiation was 94.91 % and was decreased to 91.25 % at the end of the 5th recycle. This research indicates that the self-assembled flower-like CdS nanostructure is very stable for RhB dye degradation under visible light irradiation.

Acknowledgment

The research was supported by Prince of Songkla University and Ministry of Higher Education, Science, Research and Innovation under the Reinventing University Project (Grant Number REV64038).

References

[1] X. Liu, M. Sayed, C. Bie, B. Cheng, B. Hu, J. Yu, L. Zhang, J. Materiomics **7**, 419 (2021).
[2] H. Yu, B. Huang, H. Wang, X. Yuan, L. Jiang, Z. Wu, J. Zhang, G. Zeng, J. Colloid Interface Sci. **522**, 82 (2018).
[3] Q. Li, B. Guo, J. Yu, J. Ran, B. Zhang, H. Yan, J. R. Gong, J. Am. Chem. Soc. **133**, 10878 (2011).
[4] H. Y. Wang, Z. S. Liu, L. T. Guo, H. L. Fan, X. Y. Tao, Mater. Sci. Semicond. Process **77**, 8 (2018).
[5] A. Phuruangrat, T. Sakhon, T. Thongtem, S. Thongtem, Chalcogenide Lett. **18**, 75 (2021).
[6] X. Li, Y. Wang, Y. Xie, S. Yin, R. Lau, R. Xu, Res. Chem. Intermed. **45**, 5083 (2017).
[7] W. Hussain, H. Malik, A. Bahadur, R.A. Hussain, M. Shoaib, S. Iqbal, H. Hussain, I. R. Green, A. Badshah, H. Lie, Kinet. Catal. **59**, 710 (2018).
[8] T. Senasu, S. Nanan, J. Mater. Sci. **28**, 17421 (2017).
[9] A. Phuruangrat, B. Kuntalue, T. Thongtem, S. Thongtem, Chalcogenide Lett. **16**, 149 (2019).
[10] Q. Hao, J. Xu, X. Zhuang, Q. Zhang, Q. Wan, H. Pan, X. Zhu, A. Pan, Mater. Lett. **100**, 141 (2013).
[11] S.N. Jamble, K.P. Ghoderao, R.B. Kale, Res. Chem. Intermed. **45**, 1381 (2019).
[12] D. Pathania, Sarita, B.S. Rathore, Chalcogenide Lett. **8**, 396 (2011).
[13] M. Kaur, S.K. Mehta, S.K. Kansal, J. Environ. Chemi. Eng. **6**, 3631 (2018).
[14] P.Ch. Dey, R. Das, Spectrochim. Acta A **231**, 118122 (2020).
[15] R. Chauhan, A. Kumar, R.P. Chaudhary, Res. Chem. Intermed. **39**, 645 (2013).
[16] Z. Li, H. Cheng, Y. Li, W. Zhang, Y. Yu, ACS Sustainable Chem. Eng. **7**, 4325 (2019).
[17] Powder Diffract. File, JCPDS-ICDD, 12 Campus Boulevard, Newtown Square, PA 19073–3273, U.S.A., (2001).
[18] E. A. A. Júnior, F. X. Nobre, G. S. Sousa, L. S. Cavalcante, M. R. M. Chaves Santos, F. L. Souza, J. M. E. Matos, RSC Adv. **7**, 24263 (2017).
[19] I. M. El-Nahhal, A. A. Elmanama, N. M. E. Ashgar, N. Amara, M. Selmane, M. M. Chehimi, Ultrason. Sonochem. **38**, 478 (2017).
[20] H. Zhang, D. Yang, D. Li, X. Ma, S. Li, D. Que, Cryst. Growth Des. **5**, 547 (2005).
[21] A. S. Najm, M. S. Chowdhury, F. T. Munna, P. Chelvanathan, V. Selvanathan, M. Aminuzzaman, K. Techato, N. Amin, Md. Akhtaruzzaman, Chalcogenide Lett. **17**, 537 (2020).
[22] R. K. Chava, N. Son, Y. S. Kim, M. Kang, Nanomaterials **10**, 619 (2020).
[23] C. H. Chen, Y. F. Chen, A. Shih, S. C. Lee, H. X. Jiang, Appl. Phys. Lett. **78**, 3035 (3035).
[24] S. Sa-nguanprang, A. Phuruangrat, K. Karthik, S. Thongtem, T. Thongtem, J. Aust. Ceram. Soc. **56**, 1029 (2020).
[25] A. Ramizy, M. A. Hammadi, I. M. Ibrahim, M. H. Eisa, R. Alhathlool, Dig. J. Nanomater. Bios. **11**, 1351 (2016).